



A Scara-Type 3D Printer Design And Experimental Validation

Scara Tıpi 3d Yazıcı Tasarımı ve İmali

Ahmet Saygın Öğütülmüş^{1*}, Mustafa Tınkır²

¹Ostim Technical University, 06374 Ankara, TÜRKİYE

²Necmettin Erbakan University, 42090 Konya, TÜRKİYE

Başyuru/Received: 05/10/2023

Kabul / Accepted:27/11/2023

Çevrimiçi Basım / Published Online: 31/01/2024

Son Versiyon/Final Version: 31/12/2024

Abstract

This study designed and produced a Selective Compliance Assembly Robot Arm (SCARA)-type three-dimensional Fused Deposition Modelling (FDM) printer with three degrees of freedom based on kinematic and dynamic analyses. The dynamic capability of a SCARA robot and the FDM production method were combined, and a unique printer system was obtained by using open-source software. The Kinematic Calculations were achieved by analytical methods by using geometrical equations. An open-loop control system was created by inputting forward kinematic and inverse kinematic equations to the control software. The printing processes of the Cube and Prism samples were carried out with the SCARA-type three-dimensional printer. The data obtained from the analytical calculations and the results obtained from the experiments were compared, and the error rates in the desired and obtained prints and findings that were obtained based on print quality were shared. Academic studies on SCARA in the literature have usually focused on the dynamic calculations, design and control of SCARA robots, and especially in recent years, implementation of nature-inspired algorithms. A unique printer system was obtained by using open-source software. Prints were taken from cube and prism samples, and the samples were compared to the data obtained from the analytical results. This study implemented a form of a hybrid printer model where the movement capability of a SCARA robot was combined with FDM-type three-dimensional printer production technology. The SCARA-type three-dimensional printer was produced after making kinematic and kinetic calculations.

Key Words

“SCARA, Three-dimensional printer, Kinematics, Kinetic Analysis, Design, Production”

Öz

Bu çalışmada, kinematik ve dinamik analizlere dayalı olarak üç serbestlik dereceli bir SCARA tipi üç boyutlu FDM yazıcı tasarlanmıştır ve imal edilmiştir. Bir SCARA robotunun dinamik yetenekleri ile FDM üretim yöntemi birleştirilmiş ve açık kaynaklı yazılım kullanılarak benzersiz bir yazıcı sistemi elde edilmiştir. Kinematik hesaplamalar, geometrik eşitlikler kullanılarak analitik yöntemlerle gerçekleştirilmiştir. İleri kinematik ve ters kinematik denklemleri kontrol yazılımına girilerek açık döngü kontrol sistemi oluşturulmuştur. Küp ve prizma örneklerinin baskı işlemleri SCARA tipi üç boyutlu yazıcı ile gerçekleştirilmiştir. Analitik hesaplamalardan elde edilen veriler ve deneylerden elde edilen sonuçlar karşılaştırılmış ve istenen ve elde edilen baskılardaki hata oranları ve baskı kalitesine dayalı bulgular paylaşılmıştır. Literatürdeki akademik çalışmalar genellikle SCARA robotlarının dinamik hesaplamalarına, tasarımına ve kontrolüne odaklanmıştır ve özellikle son yıllarda doğa esinli algoritmaların uygulanması üzerinde durulmuştur. Bu çalışmada bir SCARA robotunun hareket kabiliyeti, FDM tipi üç boyutlu yazıcı üretim teknolojisiyle birleştirildiği bir hibrit yazıcı modeli uygulanmıştır. SCARA tipi üç boyutlu yazıcı, kinematik ve kinetik hesaplamalar yapıldıktan sonra üretilmiştir.

Anahtar Kelimeler

“Scara, Üç boyutlu yazıcı, Kinematik, Kinetik Analiz, Tasarım, Üretim”

1. Introduction

With the developments in technology, the industry has constantly refurbished and transformed itself by going through various stages. Production based on human labor that started in the Paleolithic period with tools created out of stones, wood and animal bones is continuing today by developing on a level that exceeds the limits of the human mind with multi-purpose, advanced autonomous robots and machines equipped with artificial intelligence technology (Columbia Electronic Encyclopedia, 2000). At this point, robots are being used and making life easier in almost all aspects of life including industrial production, space research, medicine and national security (Lehoux & Grimard, 2018). SCARA, which is the first industrial robot that has its own control software and controller board, has a special place among robots. SCARA is an acronym for the expression “Selective Compliance Assembly Robotic Arm” (Kumar & Sharma, 2018). Its speed, high sensitivity, easy application, and low operation and initial investment costs are among the most important reasons for its prevalence in the industry.

Academic studies on SCARA in the literature have usually focused on the dynamic calculations, design and control of SCARA robots, and especially in recent years, implementation of nature-inspired algorithms. Das and Canan Dülger (2005) carried out mathematical modelling and dynamic simulation of a Serpent 1 model SCARA robot. They solved the motion equations of the system by using Lagrange mechanics. They simulated the system by the PD-type controller they designed and interpreted the differences in the results between real-time control and simulation. Voglewede et al. (2009) achieved the dynamic model of a 4-degree-of-freedom SCARA robot by applying the Polynomial Chaos Theory (PCT). They used the PCT methods to minimize the effects of the weight at the end of the robot effector and the weights of the robot’s own parts. Urrea and Pascal (2018) utilized the MATLAB/Simulink software to model a SCARA robot with 3 degrees of freedom by using different approaches such as the System Identification Method, Least Squares Method, Extended Kalman Filter, Adaptive Artificial Neural Networks, Genetic Algorithms and Hopfield Networks. Fister et al. (2016) designed a PID controller for a SCARA robot by using nature-inspired algorithms. They utilized evolutionary algorithms and swarm intelligence algorithms in the parameter settings of the PID. They used the differential evolutionary and genetic algorithms among evolutionary algorithms and the bat, hybrid bat, particle swarm optimization and cuckoo search optimization algorithms among the swarm-intelligence-based algorithms. They comparatively presented the results they obtained. (Weber et al., 2022) have shown that by applying the five rules for Z-Chunking, based on DFA and related principles, they generate feasible chunking configurations. (Poudel et al., 2022) In their study, presented a fully integrated and functional C3DP platform with all the necessary components and outlined how they work in harmony from a system-level perspective. Specifically, the new hardware and software architecture includes a number of new stacking strategies, a scalable timer for multi-robot printing, a SCARA-based printing robot, a mobile platform for robot transport, a modular floor tile system, and a charging station for the mobile platform, and they demonstrated the capability of the system using two case studies.

One of the most significant factors that affect the speed and efficiency in production is rapid prototyping, which is an indispensable part of design verification and product development. Prototyping may be defined as creating an ideal model before starting final production by seeing the mistakes and fixing the shortcomings step by step. Expensive and slow production of prototypes with conventional methods has led to new necessities. As a result, the ancestor of the three-dimensional printers that we use even at home today was developed in 1980s by the fused deposition modelling (FDM) production method (Gardan, 2016). Its technological infrastructure involves producing a solid, three-dimensional model of a product by stacking a raw material layer by layer by subjecting it to heat treatment or similar processes. Widespread usage of additive manufacturing today in medical applications (Zadpoor, 2017), aerospace (Yakout et al., 2017), automotive industry (Lecklider, 2017), construction (Ghaffar et al., 2018) and food industry (Lipton et al., 2015) and its implementation in new field every single day necessitated this study which was carried out with different robots and production mechanisms.

This study designed a SCARA-type three-dimensional printer by combining a SCARA robot and the FDM-type three-dimensional printer technique. The main steps that are shown in Figure 1 as CALCULATION, APPLICATION, EVALUATION and CONCLUSION were followed as the steps of the study. Design parameters such as the part dimensions for the SCARA printer and working space were determined. Kinematic and kinetic calculations were made, and mathematical modelling was carried out to allow the control of actuation and positioning in the parts. A unique printer system was obtained by using open-source software. Prints were taken from cube and prism samples, and the samples were compared to the data obtained from the analytical results.

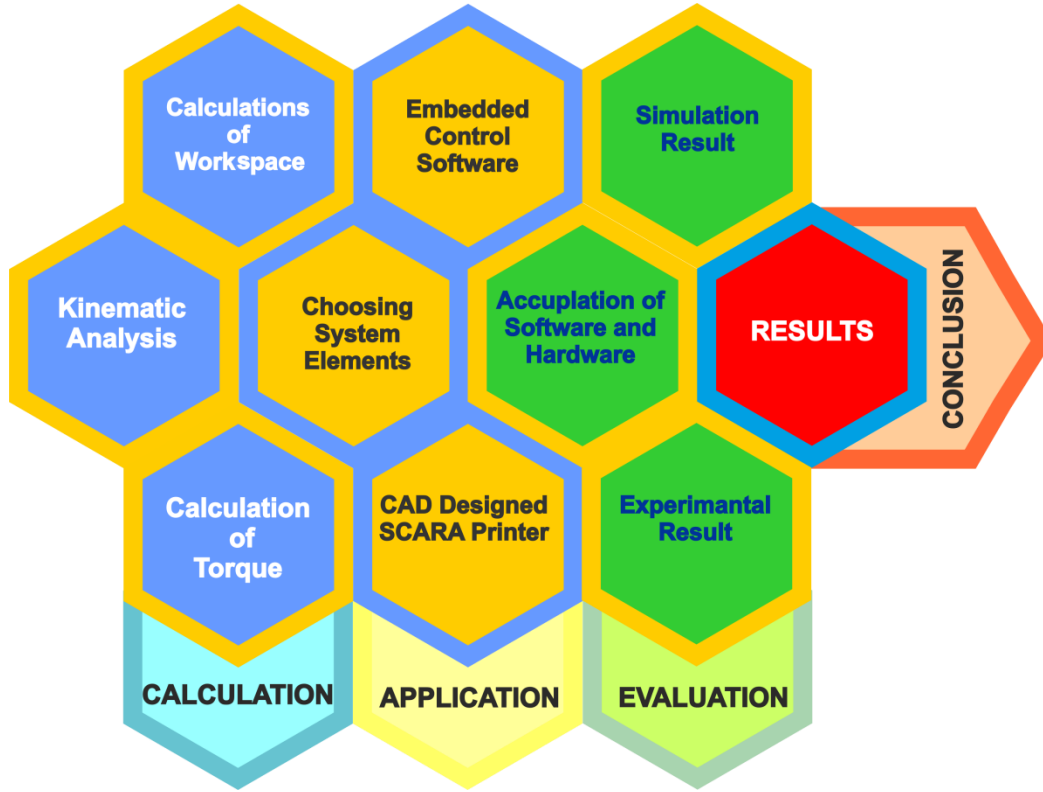


Figure 1. Schematic Diagram of Study Steps

2. Theoretical Calculations

2.1. Kinematic calculations

Kinematic analysis involves obtaining the kinematic values of the robot arm such as position, velocity and acceleration as a function of time based on a certain reference coordinate system independently of the forces and momentums that facilitate motion. It is the first step for the kinematic analysis of the robot arm. Kinematic calculations are used to mathematically model the parameters that allow determination of the force that needs to be applied on the joints for a robot manipulator to reach the desired coordinates in a certain time. At an exact time t , forward kinematics may be defined as calculation of what an exact force that is applied on the manipulator will take the arm in terms of velocity, acceleration and coordinates, while inverse kinematics may be defined as the calculation of the forces to be applied for a manipulator at exact initial coordinates to move to these exact coordinates (Figure 2). Forward and inverse kinematics calculations were obtained by analytical analysis, and they were solved by using various trigonometric equations and geometric triangular relations.

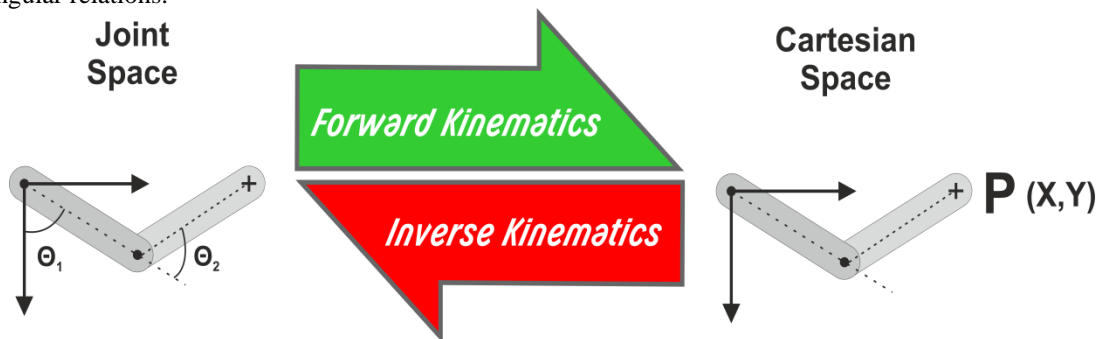


Figure 2. Kinematic Analysis Diagram

2.1.1. Forward kinematics

The coordinates of the end effector of the SCARA robot, l_1 and l_2 (Figure 3), and the projections of the arm on the vertical and horizontal axes, X and Y, were calculated by trigonometric relations as seen in Equations 2.1 and 2.2.

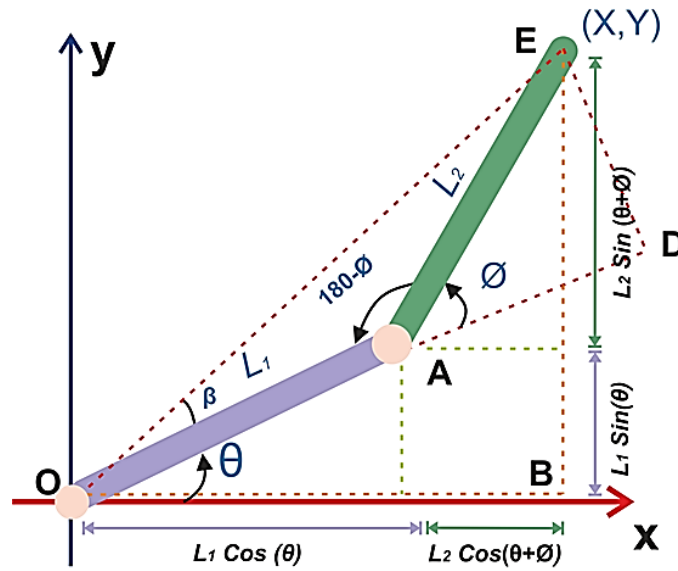


Figure 3. Position of Arms

$$X = l_1 \cos(\theta) + l_2 \cos(\theta + \phi) \tag{2.1}$$

$$Y = l_1 \sin(\theta) + l_2 \sin(\theta + \phi) \tag{2.2}$$

2.1.2. Reverse kinematics

If the cosine theorem (2.3) is applied on the triangle EAO in Figure 3 as in Equation 2.4;

$$a^2 = b^2 + c^2 - bc \cos \phi \tag{2.3}$$

$$|EO|^2 = X^2 + Y^2 = l_1^2 + l_2^2 - 2l_1l_2 \cos(180 - \phi) \tag{2.4}$$

$$l_1 = l_2$$

$$X^2 + Y^2 = 2l_1^2 + 2l_1^2 \cos(\phi)$$

$$\cos \phi = \frac{X^2 + Y^2}{2l_1^2} - 1 \tag{2.5}$$

The angle ϕ is obtained as in Equation 2.6.

$$\phi = \cos^{-1}\left(\frac{X^2 + Y^2}{2l_1^2} - 1\right) \tag{2.6}$$

If the sine of the angle ϕ isolated in Equation 2.7, Equation 2.8 is obtained.

$$(\cos \phi)^2 + (\sin \phi)^2 = 1 \tag{2.7}$$

$$\sin \phi = \sqrt{1 - (\cos \phi)^2} \tag{2.8}$$

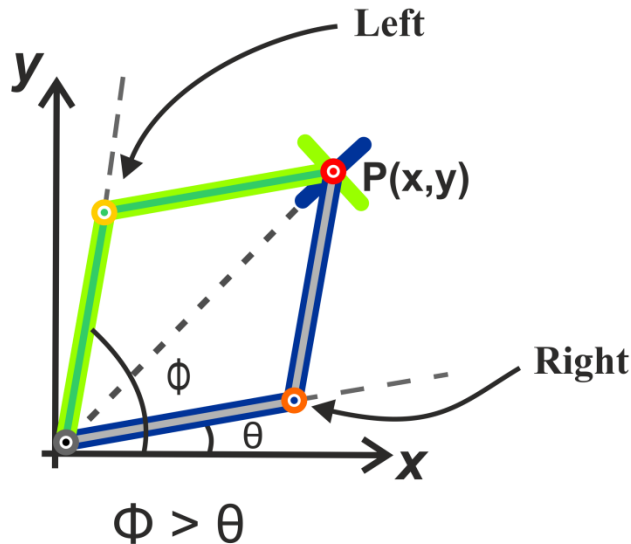


Figure 4. Different Positions of SCARA Arms

There may be multiple solutions at one point for the joint variables for the end of the robot arm. As seen in Figure 4, the printing end effector of the SCARA printer is at the same coordinates in two different positions. The joint angles may be made singular by restricting them based on a desired position. As the robot arm will start moving from a wide angle if it is moving from left to right, in order to find the angle Θ , we need to add the angle β to the angle \widehat{EOB} in Figure 3. Singularization was carried out by selecting angles based on the right-hand position in this study. Thus, to find the angle Θ , the angle β was subtracted from the angle \widehat{EOB} . To find these two angles, using Equations 2.5 and 2.8, the tangents of the triangles they formed in Figure 3 were taken.

$$|OD| = l_1 + l_2 \cos \phi$$

$$|ED| = l_2 \sin \phi$$

$$\tan \beta = \frac{|ED|}{|OD|} = \frac{l_2 \sin \phi}{l_1 + l_2 \cos \phi}$$

$$\beta = \tan^{-1}\left(\frac{l_2 \sin \phi}{l_1 + l_2 \cos \phi}\right) \quad (2.9)$$

$$\tan(\beta + \theta) = \frac{Y}{X}$$

$$\theta = \tan^{-1}\frac{Y}{X} - \beta \quad (2.10)$$

The angles of the l_1 and l_2 arms of the printer, ϕ and Θ were obtained from Equations 2.6 and 2.10.

2.2. Determining the workspace of the SCARA-type 3D printer

While determining the workspace of a SCARA-type 3D printer, it is firstly needed to determine its structural boundaries. If boundary conditions for the operation of the arm are not determined based on production, unexpected situations may be encountered. If we consider the angle β as the boundary, the general representation of the boundaries is as in Equation 2.11.

$$\begin{bmatrix} -\pi \\ -\pi + \beta \end{bmatrix} \leq \begin{bmatrix} \theta_1 \\ \theta_2 \end{bmatrix} \leq \begin{bmatrix} \pi \\ \pi - \beta \end{bmatrix} \quad (2.11)$$

A PCB hot plate with the standard dimensions of 214×214 mm was placed onto the base of the printer. Using MATLAB, the workspace of the SCARA-type printer was created, and the ideal dimensions were determined by trying different arm lengths.

The nominal workspace of the PCB is shown in Figure 5 by superimposition onto the plot. Two arm lengths were selected to be equal to each other ($l_1=l_2$) and 145 mm. The part of the hot plate with the dimensions of 145×205 mm could be used.

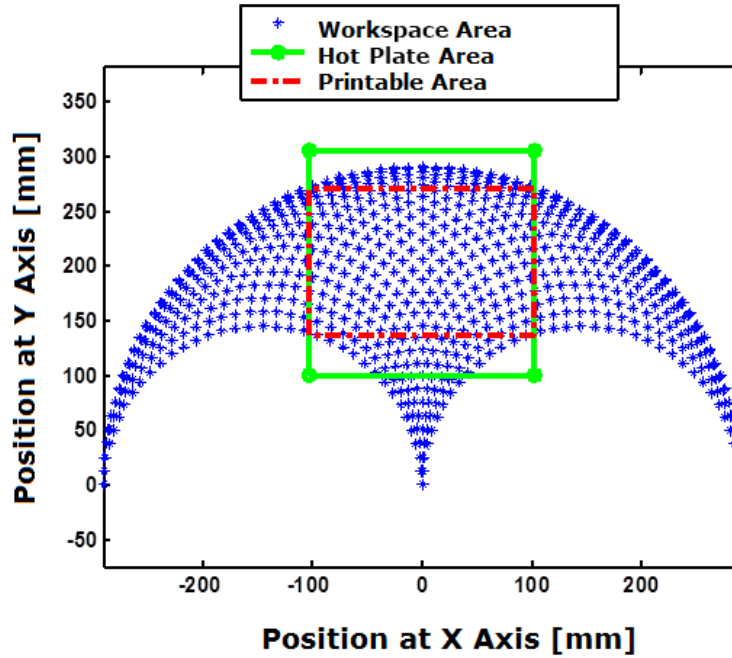


Figure 5. Comparing Printable Area and SCARA Workspace

2.3. Dynamic analysis

There are several methods for dynamic analysis such as the Lagrange-Euler (L-E), Recursive Lagrange (R-L), Newton-Euler (N-E) and Generalized D'Alembert (G-D) principles. In this study, the dynamic analysis of the robot arm involved the L-E approach which is more systematic and easier to apply in comparison to the other approaches. In the Lagrange-Euler (L-E) approach, $L = K - P$ is represented by the total energy and work in the system. For creating the Lagrange-Euler equation, we need to firstly determine the value of L (Lagrange Function) in Equation 2.12.

$$\frac{d}{dt} \left(\frac{\partial L}{\partial \dot{q}_i} \right) - \frac{\partial L}{\partial q_i} = Q_i \quad i = 1, 2, \dots, n \quad (2.12)$$

$$q = [\theta_1 \quad \theta_2]^T \quad (2.13)$$

the generalized force vector is

$$\tau = [\tau_1 \quad \tau_2]^T \quad (2.14)$$

with the torque values τ_1 and τ_2 supplied by the actuators.

For link 1, the kinetic energy is

$$K_1 = \frac{1}{2} m_1 l_1^2 \dot{\theta}_1^2 \quad (2.15)$$

And the potential energy is

$$P_1 = m_1 g l_1 \sin \theta_1 \quad (2.16)$$

For link 2,

$$x_2 = l_1 \cos \theta_1 + l_2 \cos(\theta_1 + \theta_2)$$

$$y_2 = l_1 \sin \theta_1 + l_2 \sin(\theta_1 + \theta_2)$$

so that the velocity squared is

$$v_2^2 = \dot{x}_2^2 + \dot{y}_2^2 \quad (2.17)$$

The kinetic energy for link 2 is

$$K_2 = \frac{1}{2} m_2 v_2^2$$

The potential energy for link 2 is

$$P_2 = m_2 g y_2$$

The Lagrangian function for the entire arm is

$$L = K_1 + K_2 - P_1 - P_2 \quad (2.18)$$

$$\tau_1 = \left((m_1 + m_2) l_1^2 + m_2 l_2^2 + 2m_2 l_1 l_2 \cos(\phi) \right) \ddot{\theta} + (m_2 l_2^2 + m_2 l_1 l_2 \cos(\phi)) \ddot{\phi} - m_2 l_1 l_2 (2\dot{\theta}\dot{\phi} + \dot{\theta}^2) \sin(\phi) \\ + (m_1 + m_2) g l_1 \cos(\theta) + m_2 g l_2 \cos(\theta + \phi)$$

$$\tau_2 = (m_2 l_2^2 + m_2 l_1 l_2 \cos(\phi)) \ddot{\theta} + m_2 l_1^2 \ddot{\phi} + m_2 l_1 l_2 \dot{\theta}^2 \sin(\phi) + m_2 g l_2 \cos(\theta + \phi)$$

The Manipulator dynamics are in the standard form

$$M(q)\ddot{q} + V(q, \dot{q}) + G(q) = \tau \quad (2.19)$$

Where $M(q)$ is the inertia matrix, $V(q, \dot{q})$ is the Coriolis/centripetal vector, and $G(q)$ is the gravity vector (Lewis et al., 2003).

2.4. Formation of trajectory equations

In order to simulate the data obtained from the dynamic analysis of the SCARA-type 3D printer, cubic polynomial trajectory equations were used. Cubic Polynomial Trajectories define the path between two points ($q(t_0)$ and $q(t_f)$) with a cubic polynomial

$$q(t) = a_0 + a_1 t + a_2 t^2 + a_3 t^3 \quad (2.20)$$

Differentiating Equation (2.20) velocity and acceleration can be calculated

$$\dot{q}(t) = \vartheta(t) = a_1 + 2a_2 t + 3a_3 t^2 \quad (2.21)$$

$$\ddot{q}(t) = \alpha(t) = 2a_2 + 6a_3 t \quad (2.22)$$

When the motion equations were solved by increments of 0.01 seconds with the help of the MATLAB software for the initial values of $t_0 = 0, t_f = 10; q_0 = 0, q_f = \frac{\pi}{6}; \dot{q}_0 = 0, \dot{q}_f = 0$, the position, velocity, acceleration and torque plots of the first and second arms were obtained as in Figure 6.

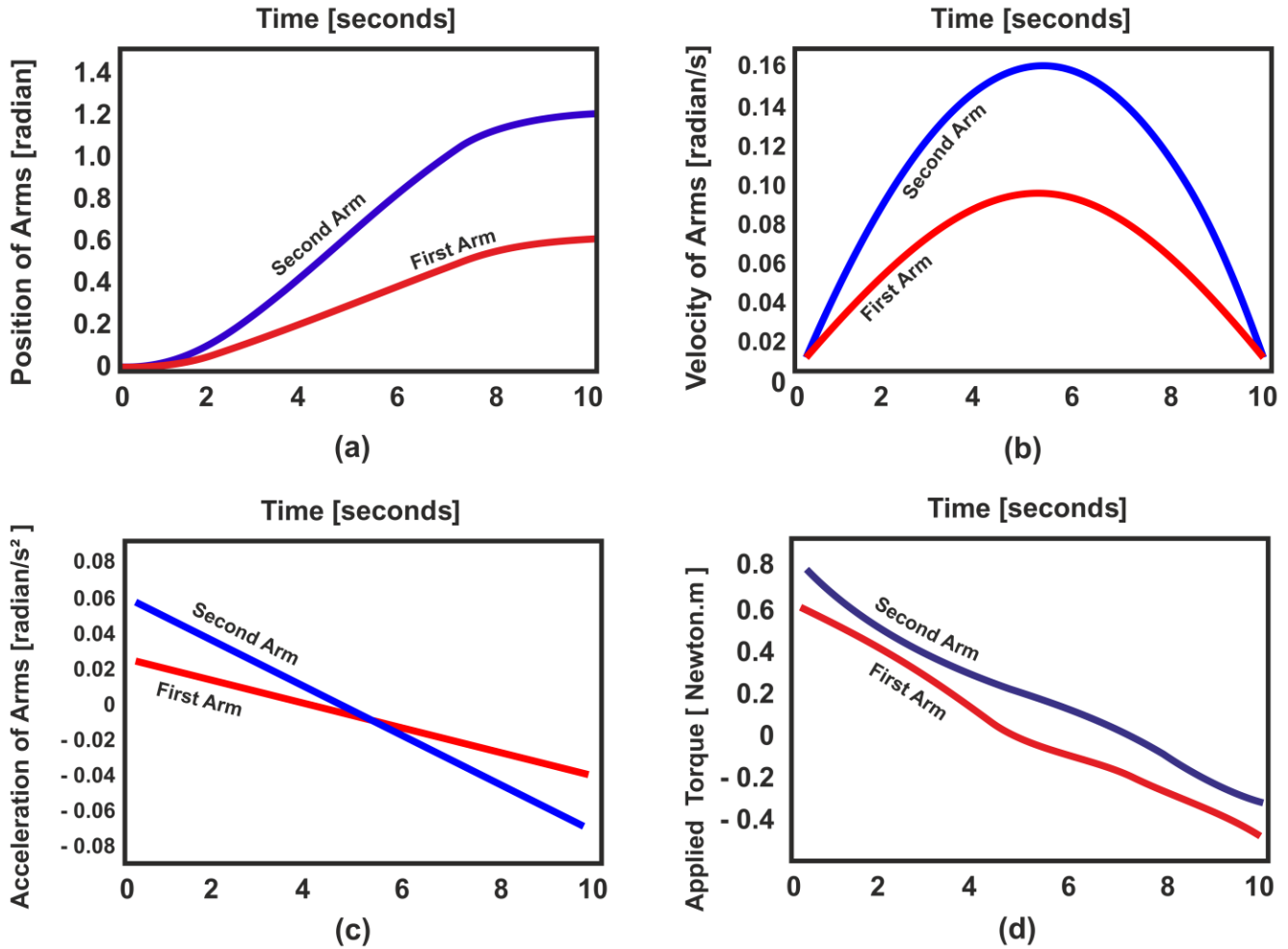


Figure 6. (a) Position (b) Velocity (c) Acceleration (d) Torque

3. SCARA 3D Printer Design

3.1. Design

As seen in Figure 7, the SCARA 3D printer was produced by three-dimensional solid modelling. The design parameters were determined by the data that were obtained from the kinematic and dynamic analyses. A simple and stable design was planned for the experimental study.

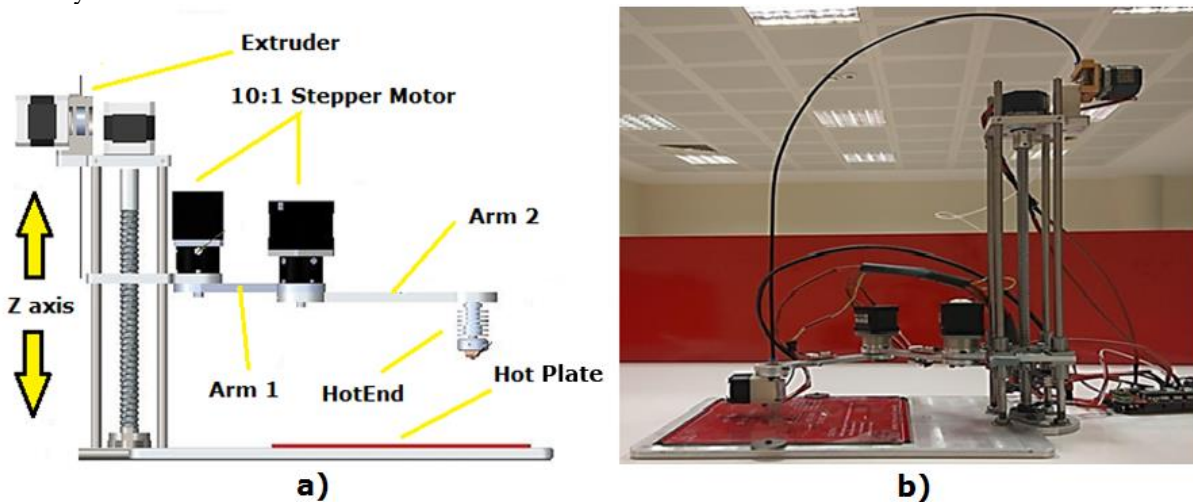


Figure 7. SCARA 3D Printer (a) CAD Design and Parts (b) Constructed View

3.2. Control system for the SCARA-type three-dimensional printer

The control system of the SCARA-type three-dimensional printer was the same as those of other three-dimensional printers, and it was an open-loop control system. The most important reason for using open-loop systems for three-dimensional printers is that they are simpler and more inexpensive. The software was adapted for the system by integrating the kinematic equations into the control software. As seen in Figure 8, the input parameters of the system were created based on the solid model to be printed, converted into torque values determined based on the rotation angles for the targeted coordinates and extracted as outputs.

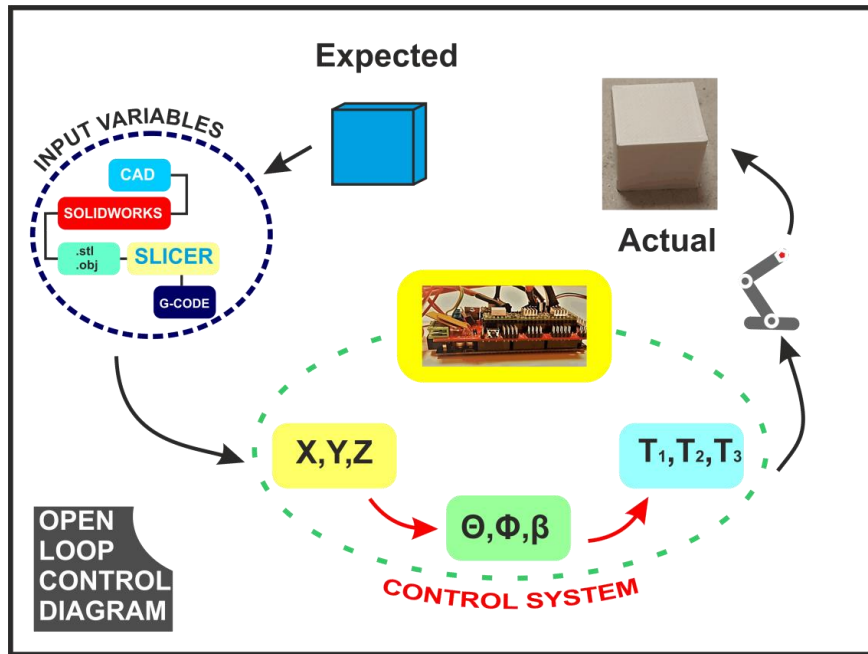


Figure 8. Open-Loop Control Diagram

4. Experimental Validation and Discussion

Table 1. SCARA Printer Specifications

Arm 1	145 mm		
Arm 2	145 mm		
Max Height	350 mm		
End Effector max length	290 mm		
Max Speed XY	40 rpm		
Max Speed Z	100 rpm		
Work Space	145 x 214 x 350 mm ³		
Gear Ratio	5:1		
Hot End Temperature	207 °C		
Hot Plate	Limits	X	Y
		-107	96
Printable Area		107	96
		107	310
		-107	310
		-107	131
		107	131
		107	276
		-107	276

The design and manufacture of the Scara type printer, whose specifications and limits are given in table 1, has been carried out. In Figure 9 trajectories consisting of the cross-section of a square prism and an equilateral triangular prism determined.

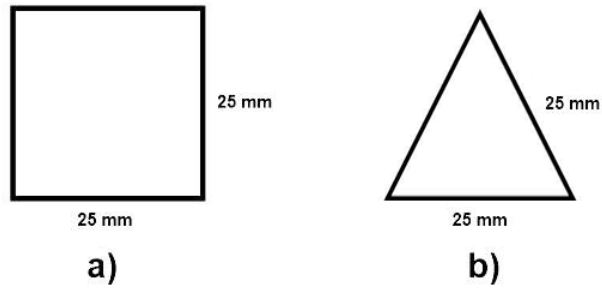


Figure 9. Dimensions of the Cross-Sections of the Prints for the (a) Square Prism and (b) Triangular Prism

Figure 10 shows the expected, simulated and actual trajectory comparison results that were obtained by the Actual Simulation obtained from the kinematic calculations based on the desired trajectory values and measurements made on the three-dimensionally printed square and triangular prisms.

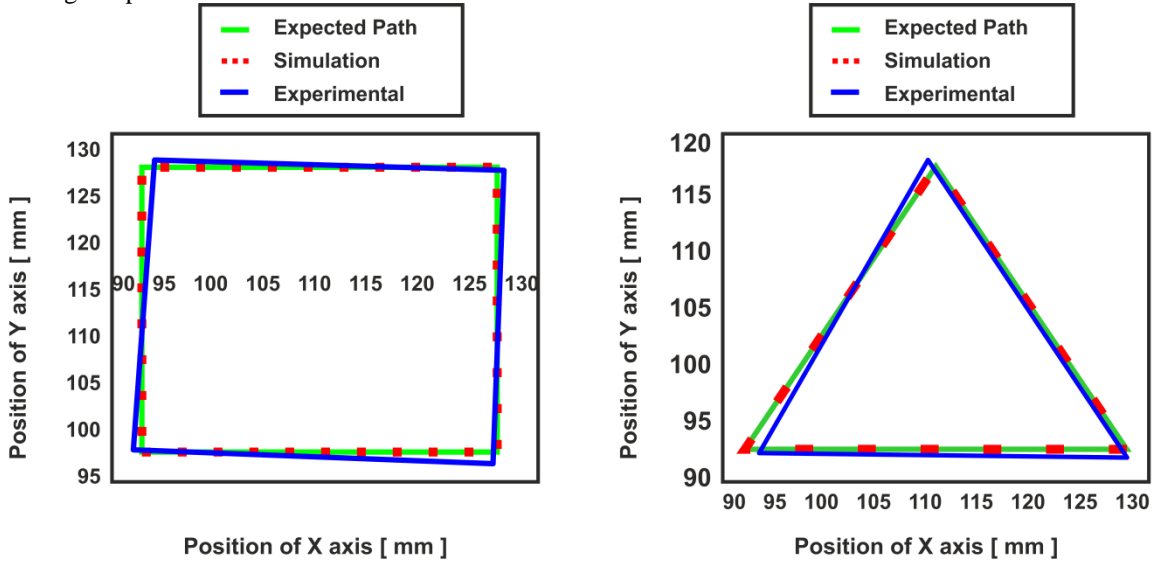


Figure 10. Expected, Simulated and Actual Trajectory Plots of the Prisms

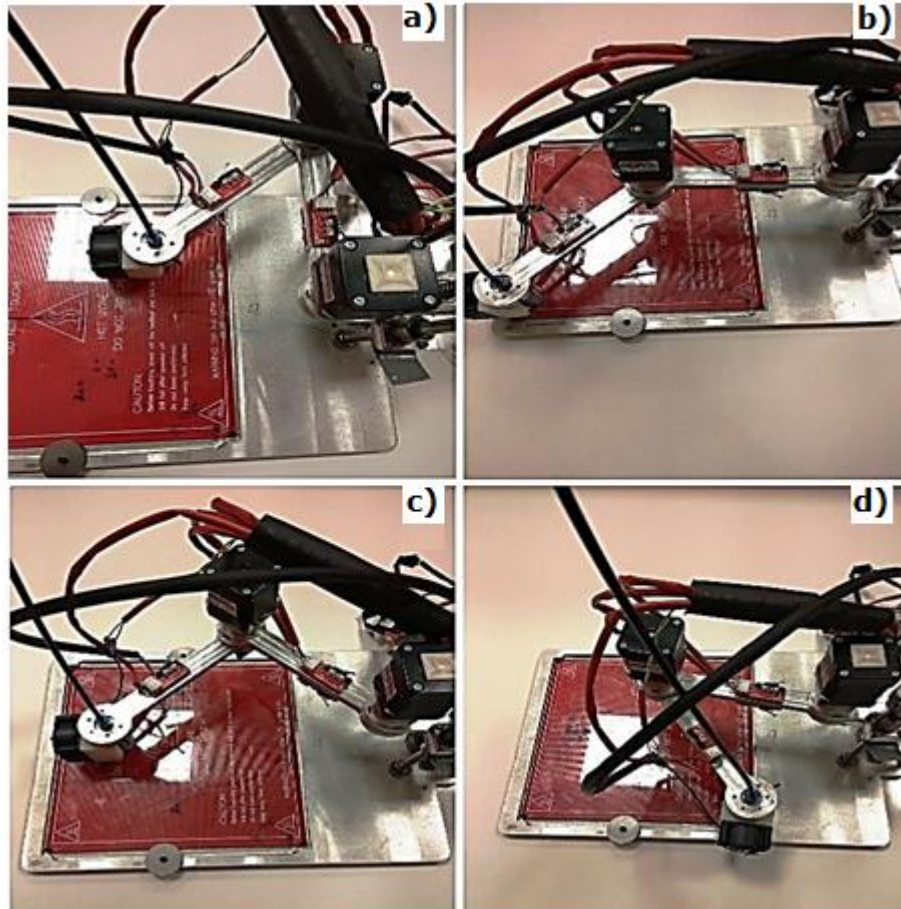


Figure 11. The Positions of the SCARA Printer from Different Angles of (a) $\Theta=0^\circ$, $\Phi=120^\circ$, (b) $\Theta=90^\circ$, $\Phi=30^\circ$ (c) $\Theta=45^\circ$, $\Phi=90^\circ$ and (d) $X=0$, $Y=0$

While the expected trajectory plot and the simulation plot corresponded to each other, there were slight deviations in the experimental plot. Figure 11 shows the positions of the arms at different angles. The kinematic calculations were verified this way. Figure 12 shows the positions of the arms during the tracking of the square and triangular trajectories independently of the Z axis.

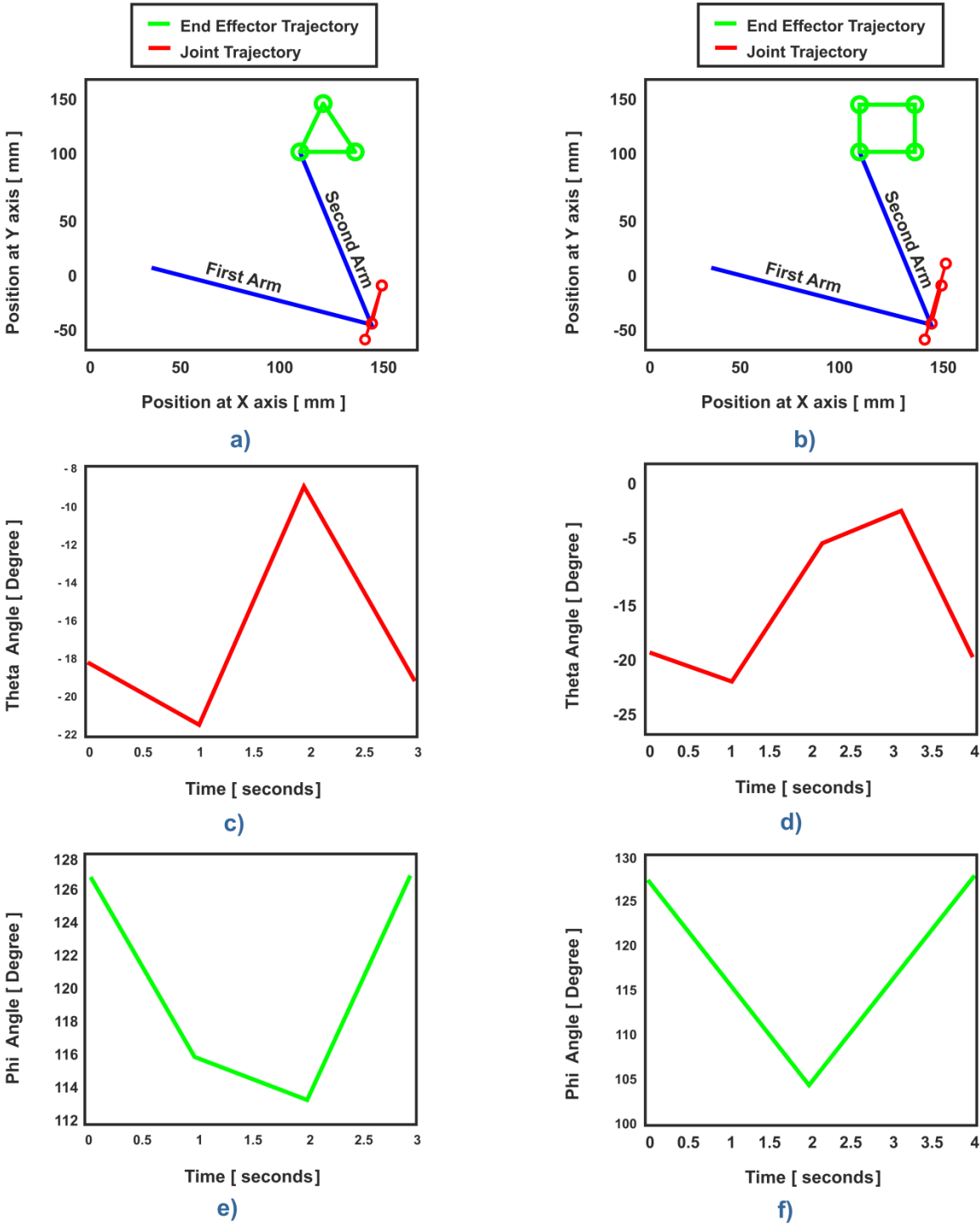


Figure 12. Positions of the Arms During Trajectory Tracking

The square and equilateral triangular prisms whose cross-section dimensions (25 mm for each edge) are given in Figure 9 were printed out by the SCARA printer as seen in Figure 13. A total of 6 random measurements were taken from each sample with a calibrated caliper, and the average of the measurement values were used. Table shows the dimensions, average measurement values and the mean error rates in the measurements for the design.

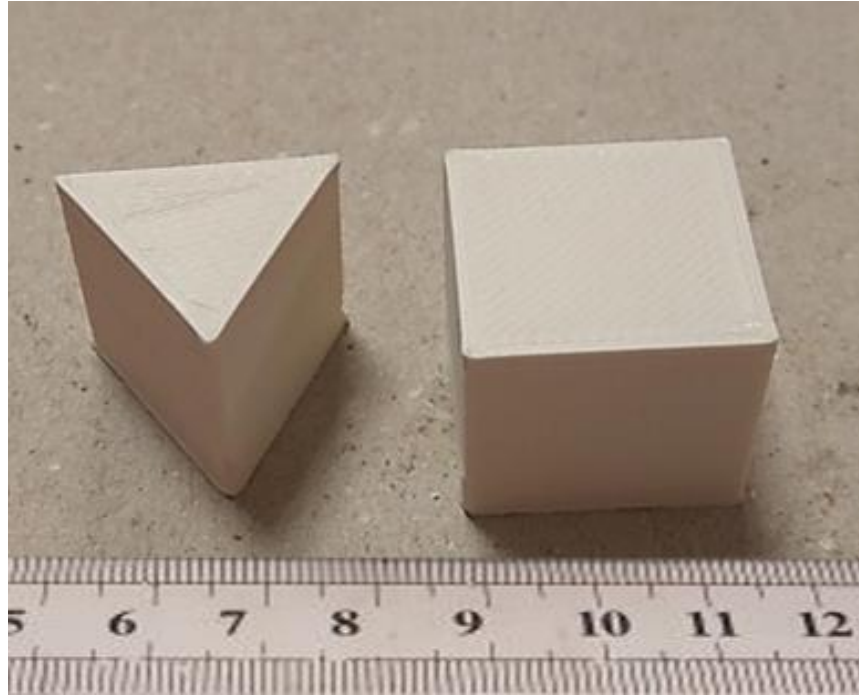


Figure 13. Print Examples Obtained with the SCARA Printer

Table 2. Comparison of the Print Samples

	Actual Measurement (mm)	Average Expected (mm)	Dimensions Error Rate (%)
Triangular Prism	26.32	25	5.28
Cube	25.87	25	3.48

Figure 14 compares the random measurements taken from the prints and the expected measurement values and presents the error rates in the measurements in percentages.

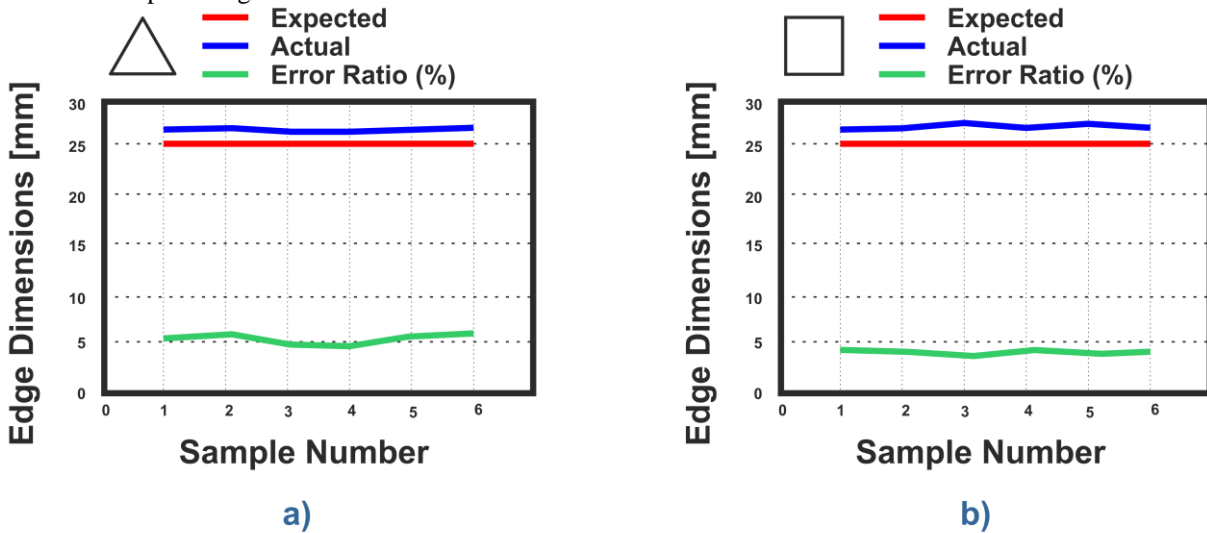


Figure 14. Comparison of Actual and Expected Measurements (a) Triangular Prism (b) Square Prism

The mean error rate in the printed triangular prism was 5.28%, while this value was 3.47% in the square prism, and there were bending values of up to 0.7 mm in radius on the corners of the prints. The reasons for these measurement errors may include the load created on the Z axis by the motor and part weights in the actuation mechanism that facilitated motion on the X and Y axes, gaps caused by the beddings or the sensitivity values of the reducers in the step motors. While there was an unusable area of 60 × 205 mm in the print effector of the SCARA manipulator in comparison to other cartesian printers in the workspace of the printer caused by blind spots that could not be reached by the print effector, 150 mm of extra working height was achieved on the Z axis in comparison to other printers.

5. Conclusions

This study implemented a form of a hybrid printer model where the movement capability of a SCARA robot was combined with FDM-type three-dimensional printer production technology. The SCARA-type three-dimensional printer was produced after making kinematic and kinetic calculations. For the SCARA-type three-dimensional printer that was completed in terms of hardware and controlled by an open-loop control system, the simulation results obtained in MATLAB and experimental results of the desired trajectories were compared, the resulting plots were presented. Consequently, when the products obtained from the hybrid printer that was designed by analytical calculations in the produced parts were examined, there were mean error rates of from 3.37% to 5.28%, it was seen that the printer was applicable and usable.

6. Further Research

Although the lengths of the arms of the SCARA-type three-dimensional printer were designed to be equal for making calculations easier, for a more efficient size of printing, the second arm may be made longer based on the workspace that is desired by up to 50%, or a third arm at the same length may be added. In order to increase the sensitivity of the system, step motors with a gearbox with higher conversion rates could be used. However, as these motors would increase the weights of the arms, they may lead to fluctuations and vibrations in motions. Instead of this servo motors with encoders and harmonic drivers that have minimal gap rates and allow closed-loop control. In addition to this, while an extra working height of 150 mm in comparison to other printers on the Z axis was achieved, as the system is not surrounded, there may be cracks and waved layers in the prints due to the temperature difference between the base and the top parts especially when ABS material is used. To prevent such an issue, as the hot plate on the base would not affect the middle layers in prints with a sufficient height, thermal insulation should be created around the printer.

References

- Columbia Electronic Encyclopedia. (2000). *Mesolithic period*. Columbia University Press. Retrieved 4 April from <http://search.ebscohost.com/login.aspx?direct=true&db=a9h&AN=134481279&lang=tr&site=ehost-live>
- Das, M. T., & Canan Dülger, L. (2005). Mathematical modelling, simulation and experimental verification of a scara robot [Article]. *Simulation Modelling Practice & Theory*, 13(3), 257-271. <https://doi.org/10.1016/j.simpat.2004.11.004>
- Fister, D., Fister, I., Jr., Fister, I., & Šafarič, R. (2016). Parameter tuning of PID controller with reactive nature-inspired algorithms [Article]. *Robotics & Autonomous Systems*, 84, 64-75. <https://doi.org/10.1016/j.robot.2016.07.005>
- Gardan, J. (2016). Additive manufacturing technologies: State of the art and trends [Article]. *International Journal of Production Research*, 54(10), 3118-3132. <https://doi.org/10.1080/00207543.2015.1115909>
- Ghaffar, S. H., Corker, J., & Fan, M. (2018). Additive manufacturing technology and its implementation in construction as an eco-innovative solution. *Automation in Construction*, 93, 1-11. <https://doi.org/https://doi.org/10.1016/j.autcon.2018.05.005>
- Kumar, A., & Sharma, R. (2018). Linguistic Lyapunov reinforcement learning control for robotic manipulators. *Neurocomputing*, 272, 84-95. <https://doi.org/https://doi.org/10.1016/j.neucom.2017.06.064>
- Lecklider, T. (2017). 3D printing drives automotive innovation [Article]. *EE: Evaluation Engineering*, 56(1), 16-19. <http://search.ebscohost.com/login.aspx?direct=true&db=a9h&AN=120540149&lang=tr&site=ehost-live>
- Lehoux, P., & Grimard, D. (2018). When robots care: Public deliberations on how technology and humans may support independent living for older adults. *Social Science & Medicine*, 211, 330-337. <https://doi.org/https://doi.org/10.1016/j.socscimed.2018.06.038>
- Lewis, F. L., Dawson, D. M., & Abdallah, C. T. (2003). *Robot Manipulator Control: Theory and Practice* (2nd ed.). CRC Press. <https://doi.org/10.1201/9780203026953>
- Lipton, J. I., Cutler, M., Nigl, F., Cohen, D., & Lipson, H. (2015). Additive manufacturing for the food industry. *Trends in Food Science & Technology*, 43(1), 114-123. <https://doi.org/https://doi.org/10.1016/j.tifs.2015.02.004>
- Poudel, L., Marques, L. G., Williams, R. A., Hyden, Z., Guerra, P., Fowler, O. L., Sha, Z., & Zhou, W. (2022). Toward Swarm Manufacturing: Architecting a Cooperative 3D Printing System. *Journal of Manufacturing Science and Engineering*, 144(8), 081004.
- Urrea, C., & Pascal, J. (2018). Design, simulation, comparison and evaluation of parameter identification methods for an industrial robot. *Computers & Electrical Engineering*, 67, 791-806. <https://doi.org/https://doi.org/10.1016/j.compeleceng.2016.09.004>
- Voglewede, P., Smith, A. H. C., & Monti, A. (2009). Dynamic performance of a SCARA robot manipulator with uncertainty using polynomial chaos theory [Article]. *IEEE Transactions on Robotics*, 25(1), 206-210. <https://doi.org/10.1109/TRO.2008.2006871>

Weber, D. H., Zhou, W., & Sha, Z. (2022). Z-Chunking for Cooperative 3D Printing of Large and Tall Objects. 2022 International Solid Freeform Fabrication Symposium,

Yakout, M., Cadamuro, A., Elbestawi, M., & Veldhuis, S. (2017). The selection of process parameters in additive manufacturing for aerospace alloys [Article]. *International Journal of Advanced Manufacturing Technology*, 92(5-8), 2081-2098. <https://doi.org/10.1007/s00170-017-0280-7>

Zadpoor, A. A. (2017). Design for additive bio-manufacturing: From patient-specific medical devices to rationally designed meta-biomaterials [Article]. *International Journal of Molecular Sciences*, 18(8), 1607. <https://doi.org/10.3390/ijms18081607>